(This is a sample cover image for this issue. The actual cover is not yet available at this time.)

Insect Biochemistry and Molecular Biology 43 (2013) 178–188

Contents lists available at SciVerse ScienceDirect

Insect Biochemistry and Molecular Biology

journal homepage: www.elsevier.com/locate/ibmb

RNAi reveals the key role of Nervana 1 in cockroach oogenesis and embryo development

Paula Irles, Fernanda A. Silva-Torres [1], Maria-Dolors Piulachs*

Institut de Biologia Evolutiva (Universitat Pompeu Fabra-CSIC), Passeig Marítim de la Barceloneta, 37, 08003 Barcelona, Spain

ARTICLE INFO

Article history:
Received 25 September 2012
Received in revised form
7 December 2012
Accepted 11 December 2012

Keywords:
Ion pump
Patency
Embryogenesis
Blattella germanica
Drosophila
Panoistic ovary

ABSTRACT

Na^+, K^+-ATPases is a heterodimer protein consisting of α- and β-subunits that control the ion transport through cell membranes. In insects the β-subunit of the Na^+, K^+-ATPase, known as Nervana, was characterized as a nervous system-specific glycoprotein antigen from adult *Drosophila melanogaster* heads. Nervana is expressed ubiquitously in all insect tissues, and in epithelial cells appeared located in a basolateral position as part of the septate junctions. Herein we study two Nervana isoforms from *Blattella germanica*, a cockroach species with panoistic ovaries. The sequencing and the phylogenetic analysis results suggest that these two isoforms are orthologs of *D. melanogaster* Nervana 1 and Nervana 2, respectively. Nervana 1 is highly expressed in the ovary of *B. germanica*, and depleting its expression results in changes in oocyte shape that do not impair oviposition. However, the resulting embryos show different defects and never hatch. These findings highlight the importance of this type of membrane pump in insect oogenesis as well as in embryo development, and its possible regulation by juvenile hormone.

1. Introduction

The flow of nutrients and metabolites through cell membranes is facilitated by ion gradients that change the cell membrane potential and contribute to the resting membrane potential, thereby serving as a driving force for the transport of materials. An important part of this ion gradient is established by Na^+ pumps which maintain the low internal Na^+ and high internal K^+ concentrations characteristic of most animal cells (Grindstaff et al., 1996). These pumps are sodium- and potassium-dependent adenosine triphosphatase (Na^+, K^+-ATPase), a plasma membrane enzyme that couples ATP hydrolysis to Na^+ and K^+ exchange against their respective chemical gradients (Kaplan, 2002).

Na^+, K^+-ATPase is a heterodimer protein consisting of α- and β-subunits present in equimolar ratios (Kaplan, 2002; Lingrel and Kuntzweiler, 1994). Multiple isoforms of both α- and β-subunits have been identified, and their number can vary among species. Thus, three isoforms of the β-subunit and two of the α-subunit have been described in the fruit fly *Drosophila melanogaster*, (Paul et al., 2007; Sun and Salvaterra, 1995b) whereas four isoforms have been reported for each subunit in humans (Kaplan, 2002; Lingrel et al., 1990). These subunits may associate into αβ-dimers in different combinations displaying distinct distribution patterns between and within tissues during ontogenesis (Lopina, 2001; Mobasheri et al., 2000). The α-subunit, which has a molecular mass of 113 kDa, shows 10 transmembrane domains containing short extracellular loops and larger cytoplasmic regions (Kaplan, 2002). A phosphorylation site in this subunit plays a major role in the catalytic function of the enzyme (Lingrel et al., 1994). The β-subunit of Na^+, K^+-ATPase, known as Nervana in *D. melanogaster*, is a glycoprotein containing a single transmembrane domain with a short amino-terminal cytoplasmic domain (around 35 residues) and a larger carboxy-terminal extracellular region that usually contains a number of glycosylation sites and three disulfide bonds (Kaplan, 2002). This β-subunit corresponds to the small subunit of the enzyme (55 kDa) and is involved in the maturation of the holoenzyme (Ackermann and Geering, 1990; Geering et al., 1989) and subsequent transport of the α-subunit to the plasma membrane (Fambrough, 1988; Noguchi et al., 1987; Takeyasu and Kawakami, 1989). In an evolutionary context, both α- and β-subunits exhibit high similarity in the conserved amino acid domains, across the entire animal kingdom (Sun et al., 1998), where gene duplication of both α- and β-subunit genes has independently led to the

* Corresponding author. Tel.: +34 932309648; fax: +34 932211011.
E-mail addresses: paula.irles@ibe.upf-csic.es (P. Irles), fastorres@usp.br (F.A. Silva-Torres), mdolors.piulachs@ibe.upf-csic.es (M.-D. Piulachs).
[1] Present address: Departamento de Biologia, Faculdade de Filosofia, Ciências e Letras de Riberão Preto, USP, Av. Bandeirantes, 3900, CEP 14040-901, Riberão Preto, SP, Brasil.

0965-1748/$ – see front matter © 2012 Elsevier Ltd. All rights reserved.
http://dx.doi.org/10.1016/j.ibmb.2012.12.003

occurrence of isoform diversity within various animal phyla (Okamura et al., 2003).

Cell volume regulation associated with potassium exchange has been observed in many cell types. In the cockroaches *Blattella germanica* and *Periplaneta americana*, for example, Kunkel (1991) and Kunkel and Faszewski (1995) highlighted the importance of ion fluxes for vitellogenin uptake and oocyte growth, and established that these fluxes may be mediated by Na^+, K^+ pumps. Similarly, in *D. melanogaster*, Bohrmann (1991) and Bohrmann and Braun (1999) used biochemical and cytochemical methods to show that changes in the volume of follicular cells are associated with variations in the extrafollicular currents pattern. Moreover, Sun and Salvaterra (1995a) purified and characterized a nervous system-specific glycoprotein antigen from adult *D. melanogaster* heads corresponding to a β-subunit of a Na^+, K^+-ATPase, and named it Nervana (nerve antigen; Nrv). These authors subsequently described the expression, localization and function of three Nervana isoforms in the nervous system of *D. melanogaster* embryos (Baumann et al., 2010; Sun and Salvaterra, 1995a, 1995b; Sun et al., 1998; Xu et al., 1999). More recently, new functions have been described for these β-subunits related to cell–cell contact (Genova and Fehon, 2003; Kometiani et al., 1998; Paul et al., 2007; Vagin et al., 2006), signal transduction (Kometiani et al., 1998) and epithelial polarity in the embryo (Laprise et al., 2009). Furthermore, roles unrelated to pump function have recently been assigned to *D. melanogaster* Nrv2. Thus, according to a study by Fehon and coworkers (Genova and Fehon, 2003; Oshima and Fehon, 2011), Nrv2 is involved in the formation of septate junctions in embryonic epithelial cells, where both subunits form a core with four proteins, coracle, neurexin, gliotactin and neuroglian, thus forming this paracellular diffusion barrier. However, although Nrv1 and Nrv2 are co-expressed in the septate junctions in a number of *D. melanogaster* tissues, Nrv1 is not required to maintain the paracellular diffusion barrier (Genova and Fehon, 2003; Paul et al., 2007).

The purpose of our work is contributing to understand oogenesis in panoistic ovaries using the cockroach *B. germanica*, a hemimetabolous insect. One characteristic of this cockroach species is that only one batch of basal follicles mature synchronously in each gonadotrophic cycle, which in our laboratory conditions lasts 7 days. At oviposition, eggs are packaged into an egg-case or ootheca that is transported by the female during 18 days, until egg hatching, and during this period the ovarian activity is arrested (Irles et al., 2009). Herein we characterize two isoforms of the β-subunit of Na^+, K^+-ATPase in the cockroach. Our phylogenetic studies suggest that the two isoforms are orthologs of *D. melanogaster* Nrv1 and Nrv2, respectively. We describe the regulatory effects of juvenile hormone (JH) upon them, whereas functional studies using RNAi approaches highlight the key role played by *B. germanica* Nervana 1 in the oogenesis of panoistic ovaries, as well in the resulting embryos that show different defects in their development and never hatch. With the aim to unveil Nervana action on embryo development, wingless and decapentaplegic expression have been measured in embryos from Nervana knockdown females. These two morphogens are important during embryogenesis determining axis development and, in case of dpp. participating in dorsal closure.

2. Materials and methods

2.1. Cockroach colony and tissue sampling

Adult females of *B. germanica* were obtained from a colony fed on Panlab dog chow and water *ad libitum*, and reared in the dark at 29 ± 1 °C and 60–70% r.h (Cruz et al., 2003). Freshly ecdysed adult females were selected and used at appropriate ages. Mated females were used in all experiments; the presence of spermatozoa in the spermatheca was assessed at the end of the experiment, indicating that mating had occurred. All dissections and tissue sampling were carried out on carbon dioxide-anaesthetized specimens, under Ringer's saline (1.8 mM $CaCl_2$, 154 mM NaCl, 2.68 mM KCl and 2.38 mM $NaHCO_3$).

2.2. Cloning of B. germanica Nervana cDNA

A 1004 bp fragment of *B. germanica* Nervana 1 (BgNrv1) was isolated from an ovarian cDNA subtractive library previously obtained (Irles et al., 2009). The fragment contains the coding region from the first methionine to poly(A) tail, but lacked the 5′ UTR. To complete it, 5′-rapid amplification of cDNA ends (RACE) was applied to RNA extracted from chorionated ovaries of 7-day-old females, using FirstChoice® RLM-RACE (Ambion, Huntingdon, Cambridgeshire, UK), according to the manufacturer's instructions. The complete ORF of *B. germanica* Nervana 2 (BgNrv2; 975 bp) was obtained from an EST library of *B. germanica* ovary obtained in the laboratory. Both, BgNrv1 and BgNrv2, were amplified, cloned into the pSTBlue-1 vector (Novagen, Madison, WI, USA) and sequenced. Primer sequences used in these experiments are detailed in Table S1.

2.3. Sequence comparisons and phylogenetic analysis

Sequences of Na^+, K^+-ATPase β subunit proteins from arthropods were retrieved from GenBank (Table S2). The search was enlarged by BLAST using the BgNrv and *D. melanogaster* Nervana proteins as queries. As outgroup, we used two Na^+, K^+-ATPase sequences from the nematode *Caenorhabditis elegans*.

Protein sequences were aligned with those obtained in *B. germanica* using the online software MAFFT (http://mafft.cbrc.jp/alignment/software/) (Katoh et al., 2002). The resulting alignment was analysed by the PHYML 3.0 program (Guindon and Gascuel, 2003) based on the maximum-likelihood principle with the amino acid substitution model. Four substitution rate categories with a gamma shape parameter of 1.444 were used. The data was bootstrapped for 100 replicates using PHYML 3.0 program.

2.4. Juvenile hormone experiments

Two different experimental approaches were used to test the response of BgNrv to juvenile hormone (JH). First, newly emerged adult females were allatectomized (Piulachs et al., 1992), three days later they were topically treated with 10 μg of JH III (Sigma) in 1 μl of acetone, and ovaries were explanted 2–4 h post-treatment. Controls were equivalently treated with acetone. The second approach involved an *in vitro* experiment using UM-BGE-1 cells derived from 4- to 5-day-old embryos of *B. germanica* (Kurtti and Brooks, 1977), which were maintained at 25 °C in Leibovitz-15 medium (Sigma, Madrid, Spain) supplemented as recommended by Munderloh and Kurtti (1989). For JH treatment, 10^6 cells ml^{-1} were seeded into 24-well cell-culture clusters (Costar, Amsterdam, The Netherlands) containing 10^{-6} M of JH III, as described previously (Maestro et al., 2005). Wells of control cells were added with the equivalent volume of acetone (1 μL). They were harvested into buffer lysis 2 and 6 h post-treatment and kept at −80 °C until processing.

2.5. RNA extraction and expression studies

Total RNA was isolated using the GenElute Mammalian Total RNA kit (Sigma). An amount of 400 ng from each RNA extraction was DNAse treated (Promega, Madison, WI, USA) and reverse

transcribed with Superscript II reverse transcriptase (Invitrogen, Carlsbad CA, USA) and random hexamers (Promega). RNA quantity and quality was estimated by spectrophotometric absorption at 260 nm/280 nm in a Nanodrop Spectrophotometer ND-1000® (NanoDrop Technologies, Wilmington, DE, USA).

Expression of BgNrv was determined by quantitative RT-PCR (qRT-PCR) in the last instar nymph and in the adult stage during the first gonadotrophic cycle. Pools of 2–6 ovary pairs for every chosen age were used. PCR primers used in qRT-PCR expression studies (Table S1) were designed using the Primer Express 2.0 software (Applied Biosystems, Foster City, CA, USA). The actin-5c gene of *B. germanica* (Accession number AJ862721) was used as a reference. PCR reactions were made using the SYBR Green Supermix (BioRad) containing 200 nM of each specific primer, and were run in triplicate. Amplification reactions were carried out at 95 °C for 2 min, and 40 cycles of 95 °C for 15 s and 60 °C for 30 s, using MyIQ Single Color RTPCR Detection System (BioRad). After the amplification phase, a dissociation curve was carried out to ensure that there was only one product (Irles et al., 2009).

Other sequences analysed during the preparation of this work were: coracle (Bgcora, accession number: HE820058), wingless (Bgwg, accession number: HE965017), decapentaplegic (Bgdpp, accession number: HE965018) and Broad-complex (BgBr-C, accession number: FN651774.1).

2.6. RNAi experiments

To knock-down BgNrv1 and assess the specificity of the phenotype, 2 different dsRNAs (dsBgNrv1A and dsBgNrv1B) were designed. The dsBgNrv1A, was a 318 bp fragment (from 509 to 826 nt) located at the middle of the ORF of the sequence; the dsBgNrv1B, was 300 bp in length (from 814 to 1113 nt), encompassed the third end of the ORF and 43 nucleotides of the 3′UTR region (Fig. S1). A 92 bp of non-coding sequence from the pSTBlue-1 vector (dsMock) was used as control dsRNA. The corresponding cDNAs were amplified by PCR and cloned into pSTBlue-1 vector. The dsRNAs were prepared as previously described (Ciudad et al., 2006). The dose used was 1 μg of dsBgNrv1A or dsBgNrv1B, and they were independently injected to newly emerged adult females in a 1 μl of saline solution. The same dose and conditions were used with dsMock-treated females.

2.7. Microscopy and histological studies

Ovaries were fixed immediately for 2 h with 4% paraformaldehyde in PBS, washed in PBT (PBS; 0.3% Triton-X100), treated with 50 μg/ml proteinase K for 2 min, washed for 2 min in 2 mg/ml glycine in PBT, washed for 10 min in PBT and fixed again for 20 min in the same solution. Embryos were fixed for 45 min with freshly prepared PEM-FA (100 mM Pipes, 2 mM EGTA, 1 mM $MgSO_4$ in 37% formaldehyde), then washed three times for 10 min with PBTB (PBS; 0.1% Triton-X100, 0.1% BSA). After three washes with PBT the tissues were saturated for 1 h at room temperature in PBTBN (PBS; 0.1% Triton-X100, 0.5% BSA and 5% normal goat serum), and incubated overnight at 4 °C in a dilution 1:50 (ovaries) or 1:10 (embryos) of the primary antibody anti-mouse Nrv5F7, developed by Sun and Salvaterra (1995a), which recognizes isoforms 1 and 2 of Nervana from *D. melanogaster* (Sun and Salvaterra, 1995a), and obtained from the Developmental Studies Hybridoma Bank. Tissues were washed with PBTBN three times and incubated for 2 h with Alexa-Fluor 488 conjugated goat antimouse IgG secondary antibody (Molecular Probes, Carlsbad, CA, USA) diluted 1:400 in PBTBN. Furthermore, ovaries were incubated for 20 min in 300 ng/ml phalloidin-TRITC (Sigma) and 5 min in 1 μg/ml DAPI (Sigma) in PBT. Embryos were incubated 5 min in 1 μg/ml DAPI (Sigma) in PBT. After three washes with PBT, tissues were mounted in Mowiol (Calbiochem, Madison, WI, USA) and observed using a Zeiss AxioImager.Z1 microscope (Apotome) (Carl Zeiss MicroImaging).

2.8. Statistics

Data are expressed as mean ± standard error of the mean (SEM). Statistical analysis between tissues samples were made by ANOVA One way, with Tukey–Kramer multiple comparison test. Statistical analyses between groups were tested by the REST 2008 program (Relative Expression Software Tool V 2.0.7; Corbett Research) (Pfaffl et al., 2002). This program makes no assumptions about the distributions, evaluating the significance of the derived results by Pair-Wise Fixed Reallocation Randomization Test tool in REST (Pfaffl et al., 2002).

3. Results

3.1. cDNA isolation and sequencing of B. germanica Nervana

Searching for JH inducible genes in the ovary, we isolated a cDNA (1004 bp) from subtractive library that matches with insect Nervana proteins. The first methionine, which is preceded by a series of in-frame stop codons, was localized 164 bases from the beginning of the sequence, and the stop codon localized 913 nucleotides from the start site. The full-length cDNA (GenBank ID: HE795995) comprises 1167 bp and encodes a protein of 304 amino acids with a predicted molecular mass of 35.15 kDa and an isoelectric point of 6.59 (Fig. S1). The 3′UTR region was found to be 89 bp long, with the polyadenylation element placed 26 nucleotides before the poly(A) tail (Fig. S1).

BLAST searches carried out using the *D. melanogaster* Nrv2 sequence upon different *B. germanica* EST libraries representing different organs and stages of development obtained in our laboratory, gave a sequence corresponding to a fragment of another Nervana protein, which we named BgNrv2. This fragment (975 bp) includes the complete ORF that encodes for a protein of 324 amino acids with a predicted molecular mass of 35.34 kDa and an isoelectric point of 6.25 (Fig. S2).

3.2. Sequence comparisons and phylogenetic analysis

The amino acid composition of BgNrv1 and BgNrv2 indicates that they are members of the conserved Na^+, K^+-ATPase β subunit superfamily, which contains a charged cytoplasmic domain, a single hydrophobic transmembrane domain between amino acids 50 and 73, and a large extracellular domain. The predicted secondary structures appeared to be very similar to that found in the two *D. melanogaster* Nervana sequences described by Sun and Salvaterra (1995b), with two potential N-glycosylation sites in positions 156 and 167 of BgNrv1 and one potential N-glycosylation sites in position 207 of BgNrv2 (Figs. S1 and S2). The first signature patterns described for β-subunit sequences in vertebrates are located in the cytoplasmic domain of both isoforms (Fig. S1 and S2). Moreover, the six conserved cysteines present in the extracellular domain and characteristic of β-subunit sequences are also present in BgNrv1 and BgNrv2 (Fig. S1 and S2).BgNrv1 and BgNrv2 share 38% of identity each other. However, a comparison of these sequences with those for other insects available in public databases leads to a highest level of identity (39%) for BgNrv1 with the termite *Coptotermes formosanus*, Nervana 1 sequence, for BgNrv2 the highest identity (60–64%) was found with the hymenopteran Nervana 2 sequences.

A maximum-likelihood analysis of arthropod Na^+, K^+-ATPase β-subunits available in the literature and databases, using the *C. elegans* Nervana proteins as outgroup, gave the tree shown in Fig. 1. This analysis distinguishes three different groups for Nervana within the Insecta clade. These three groups correspond to the three types of the β-subunit described in *D. melanogaster* as Nrv1, Nrv2 and Nrv3 (Fig. 1). Furthermore, the tree indicates that Nrv1 and Nrv2 are sister groups, whereas Nrv3 is the sister group of Nrv1+Nrv2 (Fig. 1). The topology of Nrv1, Nrv2 and Nrv3 within each node closely matches the currently accepted phylogeny of the included species. Within the Nrv2 node there are three species (*Aedes aegypti*, *Pediculus humanus* and *D. melanogaster*) with two different protein sequences each, which probably are variant isoforms (Fig. 1). The branches in the Nrv1 node are longer than in the Nrv2 and Nrv3 nodes, thus indicating a faster rate of divergence. BgNrv1 clusters in the Nrv1 node and has the sequence of *C. formosanus* as sister group, which is phylogenetically consistent given that termites are the sister group of cockroaches (Legendre et al., 2008). BgNrv2 clusters in the Nrv2 node and has a sequence of *P. humanus* as a sister group, which is also phylogenetically consistent given that this species is the only hemimetabolous insect represented in this cluster.

3.3. The ovaries of B. germanica predominantly express Nervana 1

The expression of Nervana mRNAs in *B. germanica* was studied in the following female tissues: ovary, muscle, colleterial glands, midgut, brain and fat body. Both BgNrv1 and BgNrv2 were detected in all tissues analysed, although with different degrees of expression (Fig. 2A and B). BgNrv1 is remarkably abundant in the ovary, whereas BgNrv2 is highly expressed in the brain. The high expression of BgNrv1 in the ovary suggests that the corresponding protein may be directly involved in oocyte development, while the

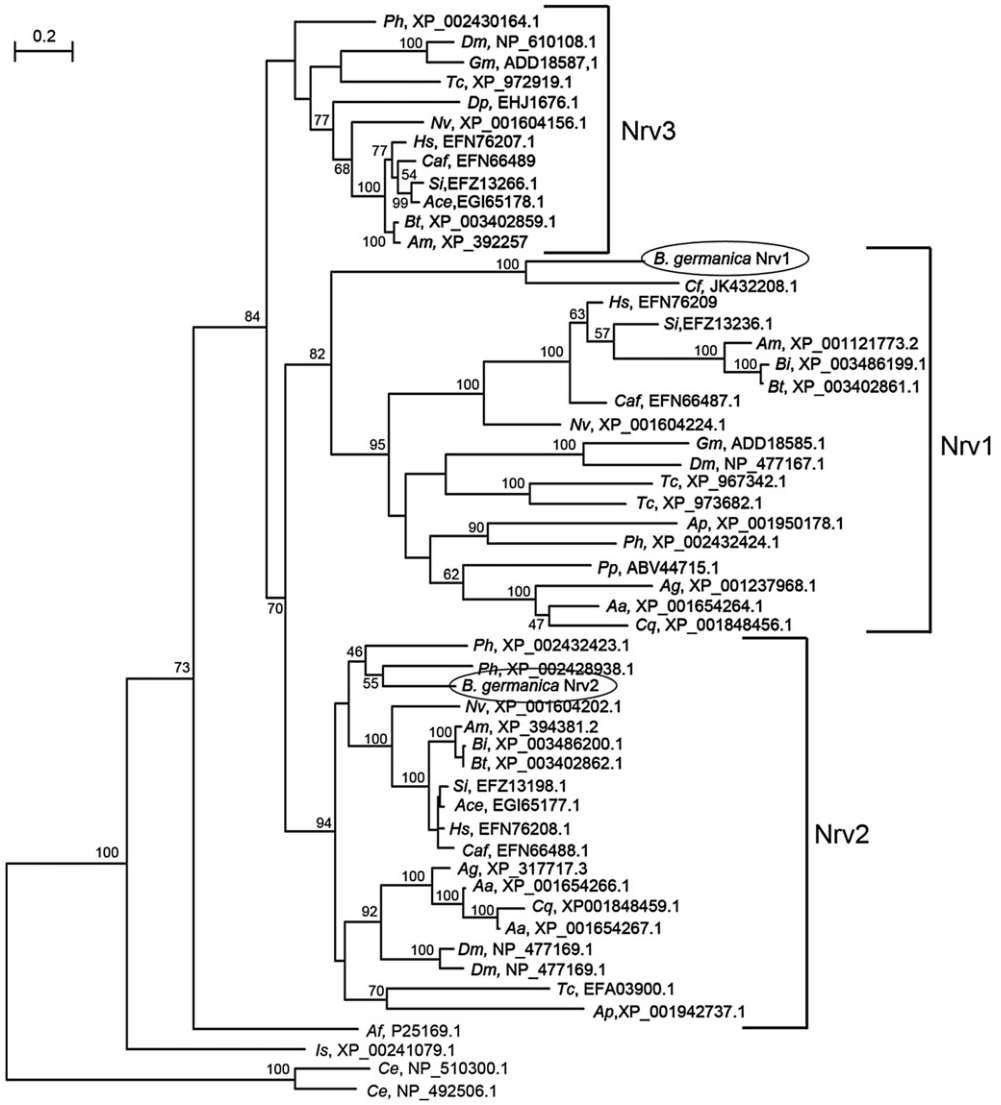

Fig. 1. Phylogenetic analysis of β subunit of Na^+, K^+-ATPase (Nervana) in insects. Tree based in the maximum-likelihood principle with the amino acid substitution model was built with the insect sequences available. The Nervana sequences of the crustacean *Artemia franciscana* (Af), the tick *Ixodes scapularis* (Is), and those of the nematode *Caenorhabditis elegans* (Ce), were used as outgroup. Bootstrap values higher than 45 are shown for the main basal nodes when. Aa: *Aedes aegypti*; Ace: *Acromyrmex echinatior*; Ag: *Anopheles gambiae*; Am: *Apis mellifera*; Ap: *Acyrthosiphon pisum*; Bi: *Bombus impatiens*; Bt: *Bombus terrestris*; Caf: *Camponotus floridanus*; Cf: *Coptotermes formosanus*; Cq: *Culex quinquefasciatus*; Dm: *Drosophila melanogaster*; Dp: *Danaus plexippus*; Hs: *Harpegnathos saltator*; Nv: *Nasonia vitripennis*; Ph: *Pediculus humanus*; Pp: *Phlebotomus papatasi*; Si: *Solenopsis invicta*; Tc: *Tribolium castaneum*.

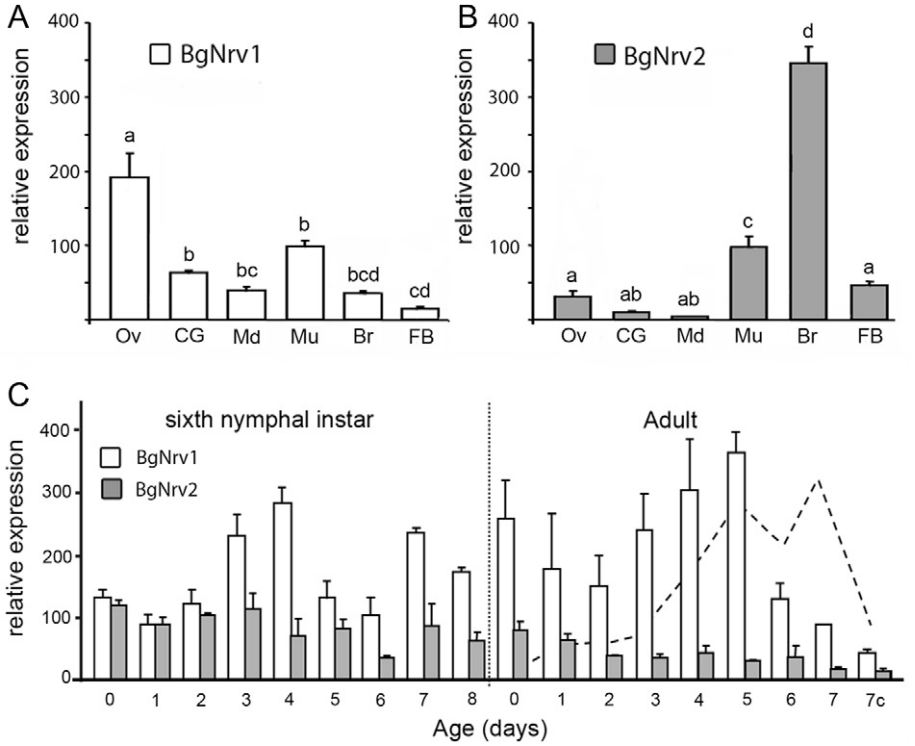

Fig. 2. Expression of *B. germanica* Nrv1 and Nrv2. (A) Expression in adult female tissues; qRT-PCR was carried out with RNA from ovary (Ov), colleterial glands (CG), midgut (Md), muscle (Mu), brain (Br) and fat body (FB). (B) Expression in the ovary during sixth nymphal instar and the first gonadotrophic cycle of adult, including ovaries from 7-day-old adult females in mid choriogenesis (7c). The profile of JH levels in the haemolymph is shown by a dashed line according to data from Treiblmayr et al. (2006). Data represent copies of mRNA per 1000 copies of actin-5c, and are expressed as the mean ± SD ($n = 3$). In A and B, different letters indicate statistically significant differences at $P < 0.01$ between samples (One-way ANOVA).

predominant expression of BgNrv2 in the brain, points to a major role in central nervous system functioning.

We then focused on ovarian tissue, and determined the mRNA levels of BgNrv1 and BgNrv2 by qRT-PCR during the sixth (last) nymphal instar (N6) and during the first gonadotrophic cycle of the adult. Results (Fig. 2C) indicate that both BgNrv1 and BgNrv2 are expressed during the entire N6 and in the adult, but with clearly higher expression levels of BgNrv1, showing an expression peak on days 3 and 4 of N6, a decrease on days 5 and 6, and a subsequent increase before the imaginal moult (Fig. 2C). The expression of BgNrv1 in the ovaries just after the imaginal moult also fluctuates, with levels starting to increase in 3-day-old females, reaching a maximum in 5-day-old females, and then decreasing dramatically to a minimum values at the end of the gonadotrophic cycle (Fig. 2C). In contrast, BgNrv2 expression in adult ovaries is very weak, even weaker than during N6 (Fig. 2C).

3.4. Expression of *B. germanica* Nervana 1 is enhanced by juvenile hormone

BgNrv1 expression in adult ovaries increases in parallel to JH titer increase (Fig. 2C), as well as to the onset of patency, or increase of intercellular spaces in the follicular epithelia (Abu-Hakima and Davey, 1975). These findings, together with the fact that the first cDNA fragment of BgNrv1 was obtained from a JH ovary subtractive library (unpublished results), suggest that JH induces or enhance BgNrv1 expression. In this line, we studied the effects of JH on BgNrv1 expression following two approaches. First, freshly emerged adult females were allatectomized (0-day-old) and treated with JH III three days later. Ovaries were collected from these allatectomized and JH-treated females between 2 and 4 h post-treatment, and BgNrv1 and BgNrv2 mRNA expression was determined. Control allatectomized females were similarly treated with acetone. BgNrv1 expression in the ovaries of allatectomized females decreased significantly (5-fold) with respect to control ovaries (Fig. 3A), whereas BgNrv1 expression levels in allatectomized females treated with JH III significantly recovered (2.9-fold), although they were still lower than those of 3-day-old control females (Fig. 3A). Conversely, allatectomized females showed an increase in BgNrv2 expression that was maintained after JH treatment (Fig. 3A). The second approach involved experiments *in vitro* using UM-BGE-1 cells, which were incubated with JH III or acetone (control) for 2 and 6 h, then harvested and processed. The expression of BgNrv1 in cells was found to be up-regulated (1.4-fold change) after incubation with JH III for 2 h, whereas BgNrv2 was unaffected by JH treatment. After 6 h in the presence of JH III both BgNrv1 and BgNrv2 expression levels were similar to those in control cells (Fig. 3B) suggesting that response of the cells to the presence of JH is fast and transient.

3.5. Nervana proteins localize in the oocyte and follicle cells of the ovary

Nervana proteins were found in both germinal and somatic cells (follicular epithelium) in ovaries from freshly emerged adult females (0-day-old; Fig. 4A and B), the labelling being clearly apparent in all ovarian follicles, from the basal to the most distal, as well as in the germarium (Fig. 4A, green signal). In 2-day-old females, the ooplasm exhibits less intense labelling (Fig. 4C and D) than that of 0-day-old females (Fig. 4B). However, the intensity of Nervana labelling increases in follicular cells (Fig. 4C and D), where it shows a typical basolateral localization, co-localizing basally with

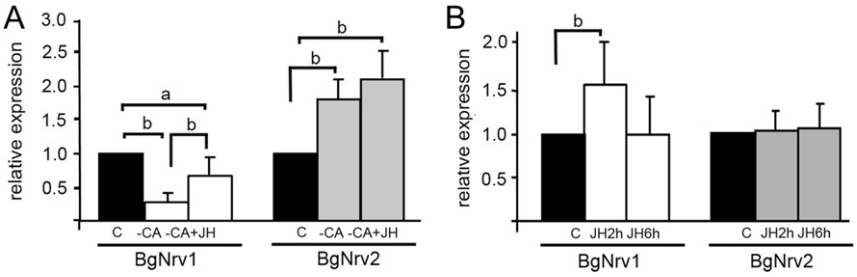

Fig. 3. *In vivo* and *in vitro* studies of JH III response on BgNrv-1 and BgNrv-2 mRNA expression. (A) Induction of Nervana mRNA expression in adult ovary by JH. Control: ovaries from 3-day-old females; −CA: 3-day-old allatectomized females; −CA + JH: 3-day-old allatectomized females that received 10 μg of JH III between 2 and 4 h before ovary dissection. (B) Induction of Nervana mRNA expression in UM-BGE-1 cells by JH. The cells were harvested at 2 and 6 h after adding JH or acetone. Actin-5c was used as reference transcript. Data represent normalized values against control (reference value = 1), and are expressed as the mean ± SD ($n = 3$), according to the Relative Expression Software Tool 2008. Letters mean significant differences (a: $P = 0.03$; b: $P = 0.0001$).

actin fibres (Fig. 4D‴). In 5-day-old females, the signal is stronger in the cytoplasm of follicular cells, increasing in the proximity of the cell membrane (Fig. 4E). Unfortunately, the large size of the full vitellogenic basal follicle at this age made impossible the observation of Nervana proteins within the oocyte.

3.6. RNAi of BgNrv1 affects basal oocyte shape, but not oviposition and ootheca formation

As BgNrv1 is the most abundant isoform in the ovary, and given that it is the only one that responds to JH treatment, we decided to

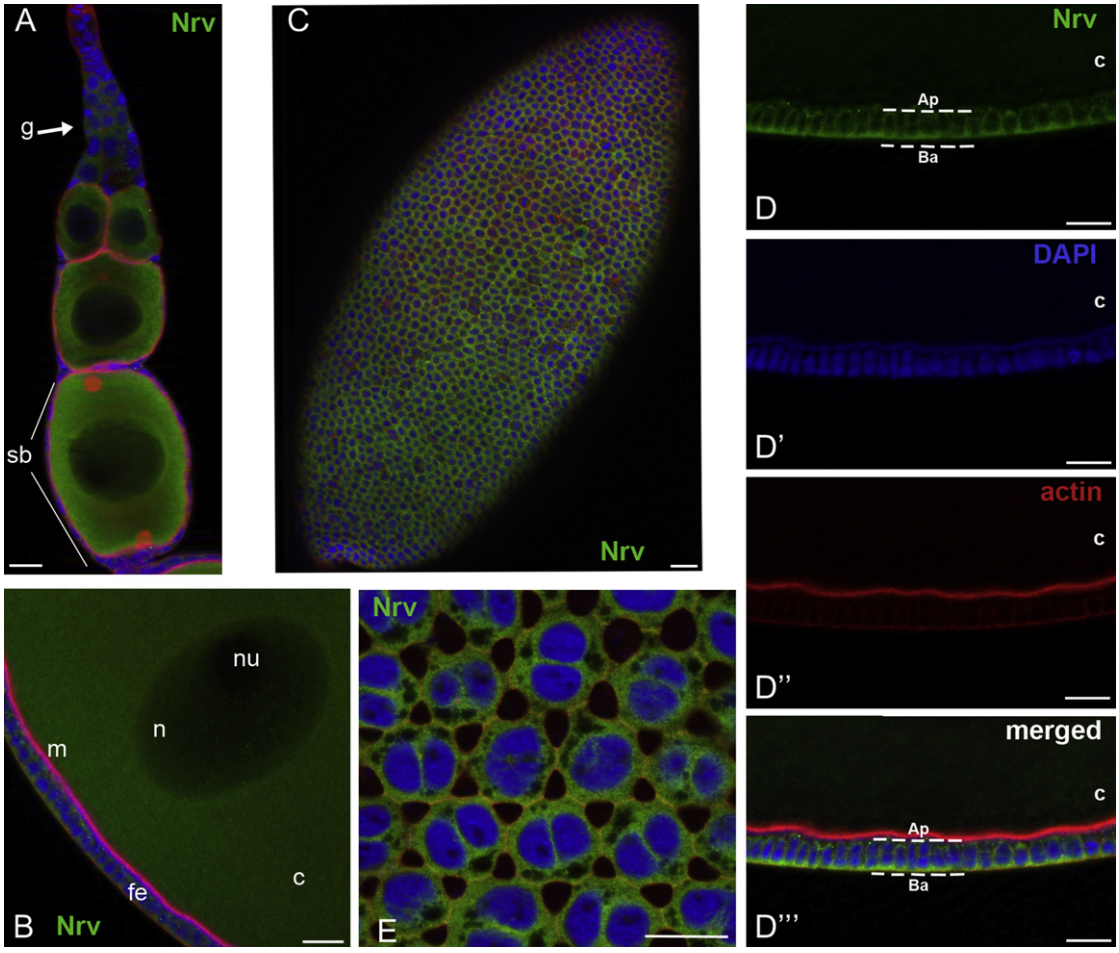

Fig. 4. Immunolocalization of Nervana proteins in ovaries from adult females. (A, B) Staining of Nervana proteins (in green) in ovarioles from freshly emerged females (0-day-old). (A) The labelling is found in the subbasal follicle (sb) and in the germarium (g). (B) Detail of basal follicle where labelling appears both in the follicular epithelia (fe) and in the germinal cell. The oocyte membrane (m) is stained with phalloidin-TRICT (red) and the labelling of Nervana (green) is found in the cytoplasm (c), but not in the nucleus (n) and nucleolus (nu). (C, D) Basal follicle from 2-day-old females. In C, a general view of the follicle, with the anterior pole oriented to the top of the image, and in D–D‴, an optical section of the basal follicle showing the distribution of Nervana in follicular cells, where it localizes basolaterally. The apical (Ap) and basal (Ba) orientation of the follicular cells is indicated. (E) Follicular cells in a basal follicle of 5-day-old females, where Nervana is concentrated in the cytoplasm (green). Nervana (green) was detected by mAb 5F7; in red: actin stained with phalloidin-TRICT; in blue: DNA stained with DAPI. Scale bars: 20 μm (For interpretation of the references to colour in this figure legend, the reader is referred to the web version of this article.).

study the function of BgNrv1 in *B. germanica* oogenesis by depleting mRNA expression with a double-strand RNA specific for BgNrv1 (dsBgNrv1). As indicated above, two dsRNAs targeting BgNrv1 were designed and synthesized. Newly emerged adult females were injected with 1 μg of dsBgNrv1 (10 females for dsBgNrv1A, and 89 females for dsBgNrv1B), whereas controls ($n = 76$) were treated equivalently with dsMock. Both dsRNAs gave the same phenotype, and the following data refer to dsBgNrv1 treatments.

Ovary dissections were performed on 5-day-old treated females, when levels of BgNrv1 mRNA expression are highest (Fig. 2B). One of the ovaries was stained to observe and describe the phenotype, whereas the other was used to measure the levels of BgNrv1 mRNA. The length of the basal follicle was found to be similar in dsMock (1.54 ± 0.03 mm) and dsBgNrv1-treated females (1.42 ± 0.11 mm; $p = 0.05$) (Fig. 5A and B). In contrast, whereas the basal follicles in dsMock females showed the typical elliptical egg-shape (Fig. 5A), the basal follicles from the ovaries of treated specimens often exhibited a pear-like shape (Fig. 5B). Despite the aspect of basal follicles, all dsBgNrv1-treated females oviposited and formed an ootheca properly; however any embryo hatched from dsBgNrv1-treated females.

Although 5-day-old ovaries from dsBgNrv1-treated females showed no major differences with respect to controls, BgNrv1 mRNA levels were 40-fold lower in dsBgNrv1-treated specimens (Fig. 5C), whereas BgNrv2 expression was similar to that in dsMock-treated controls, thus indicating that the phenotype observed is specific of BgNrv1. As Nervana is localized in septate junctions of epithelial tissues and usually coracle protein co-localizes with Nervana in these structures, Bgcora mRNA expression was measured in dsBgNrv1 treated females. Bgcora expression was found to be 5.4-fold lower (Fig. 5C) in these specimens, suggesting an affectation in cell-to-cell communication.

3.7. Nervana in embryo development

The observation that basal follicles apparently grow and matured in dsBgNrv-treated females, but embryos from these eggs do not hatch, suggest a role of Nervana in *B. germanica* embryo development. To test this conjecture, BgNrv1 and BgNrv2 expression was measured during the first six days of embryogenesis (35% of complete embryo development). The expression pattern of the two mRNAs was found to differ notably during the first 24 h, with BgNrv2 expression being 2.5-fold higher than that of BgNrv1 (Fig. 6A). From day 1 onwards, the expression levels of both isoforms decreased, with BgNrv2 being most abundant during the first hours of embryo development.

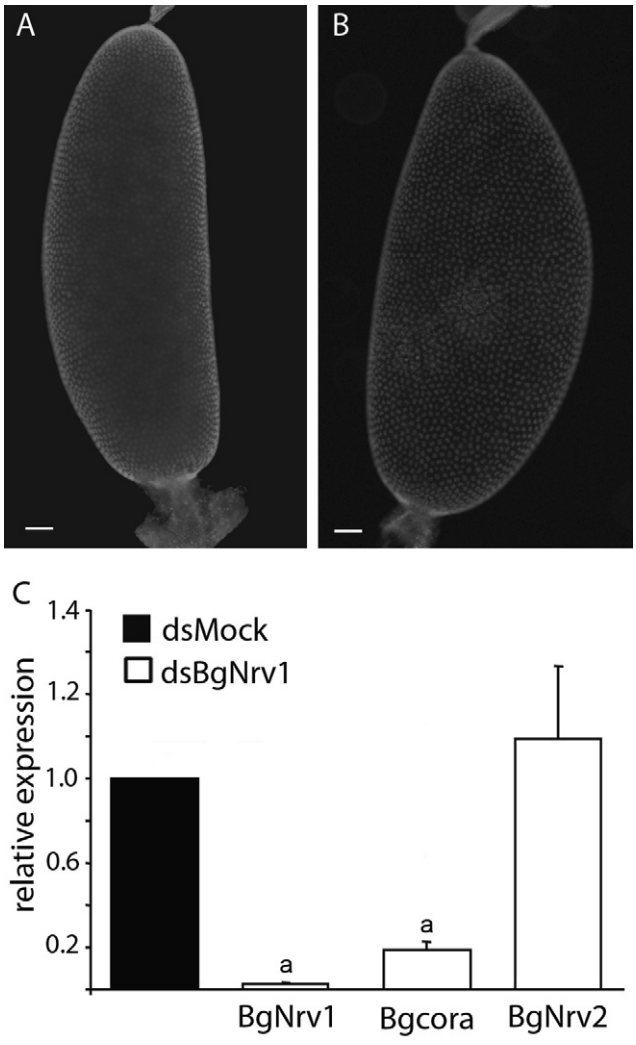

Fig. 5. Knockdown of BgNrv1 in the ovary of *B. germanica*. dsBgNrv1 was injected in newly emerged adult females and ovaries were dissected in 5-day-old adult females. (A, B) Basal follicles reach the same length in dsBgNrv1-treated females (B) than in the dsMock group (A). dsBgNrv1 follicles show a pear-like shape in contrast to the elliptical shape of dsMock-treated females. (C) Expression levels of BgNrv1, Bgcora and BgNrv2, in ovaries from 5-day-old dsMock and dsBgNrv1 groups. Data represent normalized values against control (reference value = 1), and are expressed as the mean ± SD ($n = 3$), according to the Relative Expression Software Tool 2008. Letters mean significant differences compared with respective controls ($P = 0.0001$). Scale bar: 100 μm.

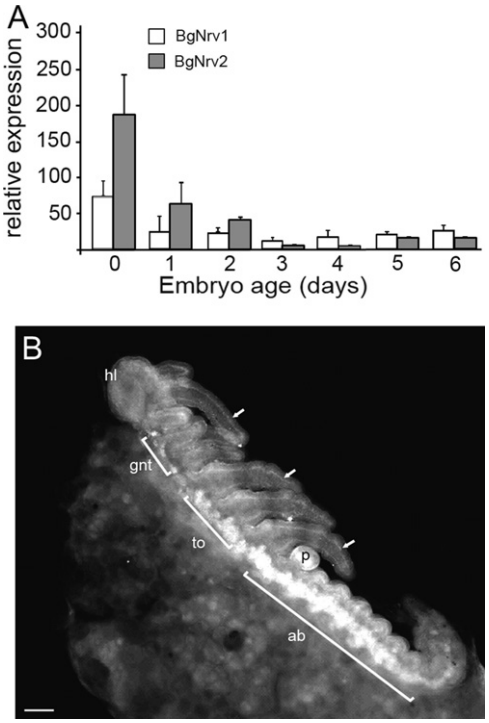

Fig. 6. Nervana in *B. germanica* embryogenesis. (A) BgNrv1 and BgNrv2 mRNA during the first six days of embryogenesis (35% of complete development). Data are expressed as copies of BgNrv mRNAs per 1000 copies of actin (mean ± SD; $n = 3$). (B) Immunolocalization of Nervana in 5-day-old *B. germanica* embryo (lateral view). The signal was detected along the ventral nerve cord and pleuropodia (p) and less intense in the head lobe (hl). Gnathal (gnt), thoracic (to) and abdominal (ab) ganglia along the nerve cord are indicated. The arrows show the labelling in the peripheral sensory neurons at the appendages. Scale bar: 100 μm.

In 5-day-old embryos, nervous system development is almost completely formed (at 30% of embryo development; Fig. 6B). At this moment, Nervana proteins are preferentially detected in both the central nervous system (CNS) and peripheral sensory neurons (PNS). Nervana labelling in the CNS appears along the ventral nerve cord, including the gnathal, thoracic and abdominal ganglia. A slightly lower degree of labelling is noticeable in the head lobes, whereas in the developing appendages it is possible to distinguish a faint staining corresponding to the PNS (Fig. 6B). In addition to the nervous system, the pleuropodia also shows intense labelling (Fig. 6B).

To study the functions of BgNrv1 in embryogenesis, we examined the parental effects of RNAi performing another set of injections of dsBgNrv1 under the same conditions as above. BgNrv1 mRNA was measured in the ovaries of these treated females at the end of oogenesis, just before oviposition, and in 1-day-old, 2-day-old and 5-day-old embryos (6%, 12% and 30% of embryo development). Before oviposition, BgNrv1 expression in the eggs from treated females was 12-fold lower (Fig. 7A, egg laying), although the ootheca was formed correctly in terms of time and general shape. As expected, the eggs from dsMock females ($n = 65$) hatched 18 ± 1 days after oviposition, with an average of 38 ± 0.8 embryos emerged per ootheca. In contrast, no embryos emerged from the oothecae formed by dsBgNrv1-treated females ($n = 78$), and 14% of females dropped the ootheca before the day 18 despite the fact that all them had mated (had spermatozoids in their spermathecae). The BgNrv1 mRNA levels in embryos from treated females decreased significantly at 6% (3.3-fold) and 12% (4.2-fold; Fig. 7A) of development, whereas expression levels in 5-day-old embryos were similar to those of dsMock-treated specimens (Fig. 7A).

To examine embryo development, oothecae were collected from dsBgNrv1 (18 oothecae; 227 embryos examined) and dsMock-treated specimens (9 oothecae; 85 embryos examined) at the 25–30% of embryo development. The embryos from dsBgNrv1-treated females showed a wide range of developmental malformations, therefore they were classified into different phenotypical categories, inspired in the criteria previously described (Piulachs et al., 2010) (category 0: embryos morphologically similar to controls; category 1: morphologically normal embryos but with a smaller abdomen; category 2: embryos arrested at 25%–30% development; category 3: amorphous mass of distinct tissue instead of a recognizable embryo; and category 4: eggs that did not manage to form the germ band). We also included two new subgroups for categories 2 and 4, namely 2a, to categorize embryos that appeared to be mis-localized, and 4a, to characterize those cases where the energids made an incipient, but very incomplete and imperfect, germinal band. The most frequent phenotype for dsBgNrv1 was that of category 2 (44% of embryos; Fig. 7B). This category included poorly developed embryos that were much smaller than those of the dsMock group (Fig. 7C) and with different

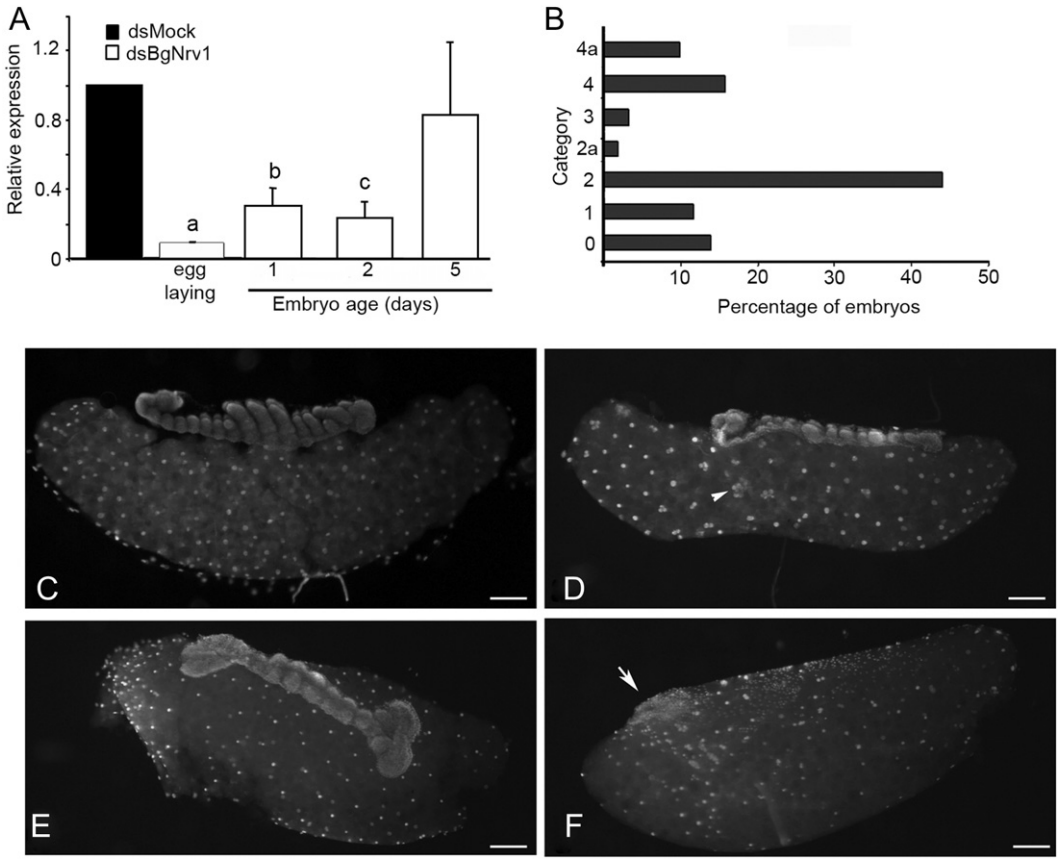

Fig. 7. Embryo development in dsBgNrv1 treated females. (A) BgNrv1 mRNA levels in 1-day-old, 2-day-old and 5-day-old embryos of dsBgNrv1 treated females (6%, 12% and 30% of embryo development). Levels of BgNrv1 in laying eggs from treated females are showed. Actin-5c expression was used as reference; data represents normalized values against respective control (reference value = 1), and expressed as the mean ± SD ($n = 3$); according to the Relative Expression Software Tool 2008. (B) Embryos at 30% of development were grouped into 7 different categories depending on their phenotype (see text). Category 2 is the most represented with more than 40% of examined embryos. (C–F) DAPI staining of dsMock (C) and dsBgNrv1 (D–F) embryos, at 30% of development (120 h). (D) Embryo poorly developed, thinner and with head shrinkage belonging to category 2. The arrowhead shows the energids clustering. (E) Mis-localized embryo corresponding to category 2a. (F) Embryo from category 4a, where the germ band is not formed and energids appear localized ventrally, in the posterior part of the egg (arrow). Embryos are oriented with the head on the right, and the ventral part in upper position. Scale bars: 0.2 mm. Letters mean significant differences compared with respective controls ($P < 0.05$).

degrees of head shrinkage (Fig. 7D). Around 1.8% of embryos did not develop in the usual ventral position and were therefore placed in category 2a (Fig. 7B and E). Similarly, 9.9% of embryos corresponded to category 4a, where the energids were dispersed by the egg plasm but only a few had regrouped around a ventral cloud, never developing a proper germ band (Fig. 7F).

Finally, 25% of embryos fell into categories 0 and 1 (Fig. 7B): they seemed correctly developed, but did not hatch at the end of embryogenesis. In a new set of experiments, we dissected 13 oothecae from dsBgNrv1-treated females 20 days after oviposition. A total of 182 embryos were analysed. Half (50%) showed the typical features of category 4 (Fig. 8A), 21% fell into category 1/20 (Piulachs et al., 2010), having completed development and exhibiting the typical distribution of bristles on the cuticle (Fig. 8B), thus resembling dsMock-embryos at 95% development. Finally, the remaining 28% exhibited arrested development at between 40% and 60% embryogenesis (Fig. 8C). We grouped all these embryos into a new category, termed 1/20a, which is characterised by complete dorsal closure and a partially hardened cuticle but with shortened appendages and no eyes.

3.8. Depletion of BgNrv1 does not affect BgBR-C or Bgwg expression, but leads to Bgdpp and Bgcora up-regulation

As the phenotypes resulting from BgNrv1 depletion in embryos are reminiscent of those obtained after depleting transcription factors of the Broad-complex (BgBR-C) family (Piulachs et al., 2010), we measured BgBR-C mRNA levels in 5-day-old embryos from dsBgNrv1-treated females. We also measured the expression of wingless (Bgwg), which participates in determining the anterior–posterior axis of the embryo, as well as decapentaplegic (Bgdpp) expression, because the role of dpp pathway in dorsal-ventral patterning. Finally, we also measured Bgcora mRNA due to its structural function in the septate junctions of epithelial tissues, where it co-localizes with Nervana. Neither BgBR-C nor Bgwins expression were significantly affected (Fig. 8D), but both Bgdpp and Bgcora were significantly up-regulated in embryos from dsBgNrv1-treated females (3.3- and 1.8-fold change, respectively; Fig. 8D). Interestingly, this up-regulation coincides in time with the recovery of BgNrv1 mRNA levels after dsRNA treatment (Fig. 7A).

4. Discussion

We have identified two β-subunit of Na^+, K^+-ATPase in *B. germanica*, which based on their sequence homology and phylogenetic analysis, have been classified as BgNrv1 and BgNrv2. Although both Nervana are ubiquitously expressed in all tissues studied, the highest expression for BgNrv1 is found in adult ovary. Conversely, BgNrv2 is preferentially expressed in nervous tissues and its presence in the ovary is very low when compared with BgNrv1 levels. This generalized expression in *B. germanica* is similar to that observed in *D. melanogaster*, where Nrv1 is broadly distributed throughout the fly but is not detected in head (Sun et al., 1998), whereas Nrv2 is the most abundant with a specific nervous system distribution (Sun and Salvaterra, 1995a, 1995b; Sun et al., 1998). Both proteins have an overlapping yet distinctive distribution with Nrv3, which is enriched in the eye (Baumann et al., 2010). A number of mammalian species also contain multiple forms of β-subunits that are expressed in characteristic cell- and tissue type-specific patterns related to the different roles described for each isoform (Blanco and Mercer, 1998; Grindstaff et al., 1996; Shyjan et al., 1990a, 1990b; Shyjan and Levenson, 1989; Watts et al., 1991).

Although the enzymatic activity of ATPases has been studied in the ovarian follicle of *D. melanogaster* (Bohrmann and Braun, 1999), this is the first time that expression of an Na^+, K^+-ATPase β-subunit has been described in ovarian tissue. In the panoistic ovary of *B. germanica*, BgNrv proteins are detected in both the oocyte and follicular cells. In later tissue, Nervana proteins are localized basolaterally, which is a characteristic position in epithelial cells (Cereijido et al., 2008; Paul et al., 2007).

The mRNA levels of BgNrv1 in adult ovaries follow an expression pattern similar to that of JH levels in the haemolymph (Treiblmayr et al., 2006). In addition, the positive response of BgNrv1 mRNA to JH suggests a connexion between the enzyme and this hormone. This possible regulation of an Na^+, K^+-ATPase by JH was first proposed some years ago for *Rhodnius prolixus* (Ilenchuk and Davey, 1987), *Locusta migratoria* (Sevala and Davey, 1989) and *Heliothis*

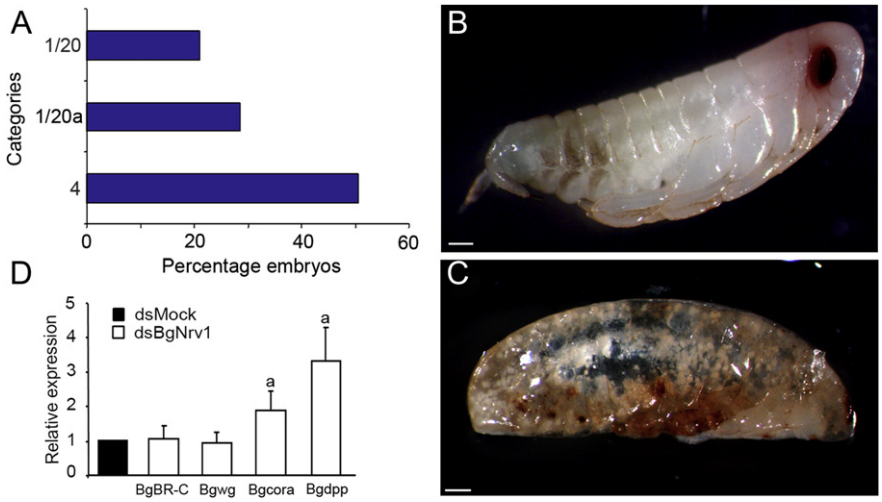

Fig. 8. Embryo development in dsBgNrv1-treated females after 20 days of ootheca transport. (A) Embryos were distributed in three categories (see text) matching mostly in the class 4. (B) dsBgNrv1 embryo corresponding to category 1/20, resembling to control (dsMock-treated) embryo, but failed to hatch. (C) dsBgNrv1 embryo that arrested development at 40–60% of embryogenesis (category 1/20a), with short appendages and lacking eyes. Scale bars: 0.2 mm. (D) Expression of BgBR-C, Bgwg, Bgcora and Bgdpp in BgNrv1 knockdown 5-day-old embryos. BgBR-C and Bgwg mRNA levels are similar to those of dsMock, but Bgcora and Bgdpp are up-regulated by 1.8 and 3.3 fold, respectively. Actin-5c expression was used as reference; data represents normalized values against respective control (reference value = 1), and expressed as the mean ± SD ($n = 3$); according to the Relative Expression Software Tool 2008. Letters mean significant differences compared with respective controls ($P = 0.001$).

virescens (Pszczolkowski et al., 2005) in relation to the patency regulation in follicular cells, thus suggesting that the reduction in cell volume could occur as a result of ion exchange between the cell and the extracellular media. In the ovary of *D. melanogaster*, where vitellogenesis is controlled by 20-hydroxyecdysone, this hormone modifies ATPase activation (Bohrmann, 1991). Despite these previous findings, silencing of Nervana in *B. germanica* did not impair patency, thereby suggesting that BgNrv1 is not involved in this process and therefore another ion pump, such the H^+V-ATPase that coordinates ion exchange in insect oocytes and allow vitellogenin uptake by the oocyte membrane (Harvey et al., 1998; Janssen et al., 1995; O'Donnell and Sharda, 1994), could be the responsible for this function.

However, although the only phenotype detected in the ovary was a change in the volume and shape of the oocyte, embryo development was severely affected given that no embryos emerged after BgNrv1 depletion. This effect on embryo development suggests that dsBgNrv1 is incorporated into the egg and transmitted to the embryo, as indicated by the low levels of BgNrv1 mRNA in the first hours of embryo development prior to activation of the zygotic genes (Piulachs et al., 2010). Both Bgdpp and Bgcora were up-regulated in BgNrv1 knockdown embryos, whereas BgBR-C levels were unaffected. These results confirm that, despite the similarity of the embryo phenotype with that found in females treated with dsBgBR-C (Piulachs et al., 2010), the results obtained are not dependent on BgBR-C but directly dependent on BgNrv1.

Cora has been described in *D. melanogaster* as a septate junction marker (Fehon et al., 1994; Genova and Fehon, 2003; Lamb et al., 1998; Ward et al., 1998), and also as a member of the epithelial polarity protein family, together with Yurt and the membrane proteins Neurexin IV and Na^+, K^+-ATPase (Laprise et al., 2009). In agreement with the proposed interaction between this protein and Nervana (Genova and Fehon, 2003), Bgcora mRNA was down-regulated in ovaries from BgNrv1 knockdowns, thus suggesting that septate junction organization was affected, probably as a result of the mis-localization of coracle protein (Paul et al., 2007). In embryos from dsBgNrv1-treated females, Bgcora mRNA was up-regulated in parallel with the recovering of BgNrv1 mRNA expression, suggesting a rapid transcription of Bgcora in response to BgNrv-1 levels. In *D. melanogaster* the role of dpp has been thoroughly described in either dorsal-ventral patterning (Biemar et al., 2006; Eldar et al., 2002) or in the dorsal closure event, activating cell elongation and differentiation (García-Fernández et al., 2007; Martín-Blanco et al., 1998; Zeitlinger et al., 1997). The dorsal closure is a morphogenetic process, while epidermal and amnioserosa cells engage in a sequence of coordinated cell shape changes and epithelial movements, thus creating epidermal continuity (Harden, 2002). In *B. germanica*, the dorsal organ is visible around 35% of embryo development (120 h) and two days later (40% total development) the dorsal closure of the body wall is completed (Piulachs et al., 2010). The up-regulation of Bgdpp in dsBgNrv-1 embryos at 35% of development suggests an indirect effect of BgNrv1 in the dorsal closure process, through mechanisms that would require further studies.

The importance of BgNrv1 in *B. germanica* oogenesis is clear. In BgNrv1 depleted specimens the shape of the oocyte is altered during the first gonadotrophic cycle, and resulting eggs show a range of embryo malformations, from failing to form the germ band to almost completely formed embryos that are unable to hatch. These changes reflect failures in different stages of embryo development. The diversity of phenotypes observed is probably due to disorganization of the septate junction resulting from an effect on the epithelial polarity protein coracle. Therefore, septate junction formation appears to be crucial in practically all stages of embryogenesis.

Acknowledgements

This work was supported by the Ministry of Science and Innovation, Spain (projects BFU2008-00484 and BFU2011-22404 to MDP), and by the CSIC (grant 2010TW0019, Formosa program). PI is recipient of a postdoctoral research grant (BECAS CHILE) from the "Comisión Nacional de Investigación Científica y Tecnológica" (CONICYT, Chile). FAST was supported by a fellowship from FAPESP, to do a stage in the IBE. We are grateful to Prof. Xavier Bellés for helpful scientific discussions and critical comments on the manuscript. Thanks are also due to Dr Timothy Kurtti (University of Minnesota, USA) for providing the UM-BGE-1 cell line. The monoclonal antibody Nrv5F7 developed by Paul M. Salvaterra was obtained from the Developmental Studies Hybridoma Bank developed under the auspices of the NICHD and maintained by The University of Iowa, Department of Biology, Iowa City, IA 52242.

Appendix A. Supplementary data

Supplementary data related to this article can be found at http://dx.doi.org/10.1016/j.ibmb.2012.12.003.

References

Abu-Hakima, R., Davey, K.G., 1975. Two actions of juvenile hormone on the follicle cells of Rhodnius prolixus Stal. Can. J. Zool. 53, 1187–1188.
Ackermann, U., Geering, K., 1990. Mutual dependence of Na, K-ATPase alpha- and beta-subunits for correct posttranslational processing and intracellular transport. FEBS Lett. 269, 105–108.
Baumann, O., Salvaterra, P.M., Takeyasu, K., 2010. Developmental changes in beta-subunit composition of Na, K-ATPase in the Drosophila eye. Cell. Tissue Res. 340, 215–228.
Biemar, F., Nix, D.A., Piel, J., Peterson, B., Ronshaugen, M., Sementchenko, V., Bell, I., Manak, J.R., Levine, M.S., 2006. Comprehensive identification of Drosophila dorsal-ventral patterning genes using a whole-genome tiling array. Proc. Natl. Acad. Sci. U S A 103, 12763–12768.
Blanco, G., Mercer, R.W., 1998. Isozymes of the Na-K-ATPase: heterogeneity in structure, diversity in function. Am. J. Phys. 275, F633–F650.
Bohrmann, J., 1991. Potassium uptake into Drosophila ovarian follicles: relevance to physiological and developmental processes. J. Insect Physiol. 37, 937–946.
Bohrmann, J., Braun, B., 1999. Na, K-ATPase and V-ATPase in ovarian follicles of Drosophila melanogaster. Biol. Cell. 91, 85–98.
Cereijido, M., Contreras, R.G., Shoshani, L., Flores-Benitez, D., Larre, I., 2008. Tight junction and polarity interaction in the transporting epithelial phenotype. Biochim. Biophys. Acta 1778, 770–793.
Ciudad, L., Piulachs, M.D., Belles, X., 2006. Systemic RNAi of the cockroach vitellogenin receptor results in a phenotype similar to that of the Drosophila yolkless mutant. Febs J. 273, 325–335.
Cruz, J., Martin, D., Pascual, N., Maestro, J.L., Piulachs, M.D., Belles, X., 2003. Quantity does matter. Juvenile hormone and the onset of vitellogenesis in the German cockroach. Insect Biochem. Mol. Biol. 33, 1219–1225.
Eldar, A., Dorfman, R., Weiss, D., Ashe, H., Shilo, B.Z., Barkai, N., 2002. Robustness of the BMP morphogen gradient in Drosophila embryonic patterning. Nature 419, 304–308.
Fambrough, D.M., 1988. The sodium pump becomes a family. Trends Neurosci. 11, 325–328.
Fehon, R.G., Dawson, I.A., Artavanis-Tsakonas, S., 1994. A Drosophila homologue of membrane-skeleton protein 4.1 is associated with septate junctions and is encoded by the coracle gene. Development 120, 545–557.
García-Fernández, B., Martinez Arias, A., Jacinto, A., 2007. Dpp signalling orchestrates dorsal closure by regulating cell shape changes both in the amnioserosa and in the epidermis. Mech. Dev. 124, 884–897.
Geering, K., Theulaz, I., Verrey, F., Hauptle, M.T., Rossier, B.C., 1989. A role for the beta-subunit in the expression of functional Na^+–K^+-ATPase in Xenopus oocytes. Am. J. Physiol. 257, C851–C858.
Genova, J.L., Fehon, R.G., 2003. Neuroglian, Gliotactin, and the Na^+/K^+ ATPase are essential for septate junction function in Drosophila. J. Cell. Biol. 161, 979–989.
Grindstaff, K.K., Blanco, G., Mercer, R.W., 1996. Translational regulation of Na, K-ATPase alpha1 and beta1 polypeptide expression in epithelial cells. J. Biol. Chem. 271, 23211–23221.
Guindon, S., Gascuel, O., 2003. A simple, fast, and accurate algorithm to estimate large phylogenies by maximum likelihood. Syst. Biol. 52, 696–704.
Harden, N., 2002. Signaling pathways directing the movement and fusion of epithelial sheets: lessons from dorsal closure in Drosophila. Differentiation 70, 181–203.

Harvey, W.R., Simon, H.P., Maddrell, S., Telfer, W., Wieczorek, H., 1998. H^+ V-ATPases energize animal plasma membranes for secretion and absorption of ions and fluids. Am. Zool. 38, 426–441.

Ilenchuk, T.T., Davey, K.G., 1987. Effects of various compounds on Na/K-ATPase activity, JH I binding capacity and patency response in follicles of *Rhodnius prolixus*. Insect Biochem. 17, 1085–1088.

Irles, P., Belles, X., Piulachs, M.D., 2009. Identifying genes related to choriogenesis in insect panoistic ovaries by Suppression Subtractive Hybridization. BMC Genomics 10, 206.

Janssen, I., Hendrickx, K., Klein, U., De Loof, A., 1995. Immunolocalization of a proton V-ATPase in ovarian follicles of the tobacco hornworm Manduca sexta. Arch. Insect Biochem. Physiol. 28, 131–141.

Kaplan, J.H., 2002. Biochemistry of Na, K-ATPase. Annu. Rev. Biochem. 71, 511–535.

Katoh, K., Misawa, K., Kuma, K., Miyata, T., 2002. MAFFT: a novel method for rapid multiple sequence alignment based on fast Fourier transform. Nucleic Acids Res. 30, 3059–3066.

Kometiani, P., Li, J., Gnudi, L., Kahn, B.B., Askari, A., Xie, Z., 1998. Multiple signal transduction pathways link Na^+/K^+-ATPase to growth-related genes in cardiac myocytes. The roles of Ras and mitogen-activated protein kinases. J. Biol. Chem. 273, 15249–15256.

Kunkel, J.G., 1991. Models of pattern formation in insect oocytes. In Vivo 5, 443–456.

Kunkel, J.G., Faszewski, E., 1995. Pattern of potassium ion and proton currents in the ovariole of the cockroach, Periplaneta americana, indicates future embryonic polarity. Biol. Bull. 189, 197–198.

Kurtti, T.J., Brooks, M.A., 1977. Isolation of cell lines from embryos of the cockroach, Blattella germanica. In Vitro 13, 11–17.

Lamb, R.S., Ward, R.E., Schweizer, L., Fehon, R.G., 1998. Drosophila coracle, a member of the protein 4.1 superfamily, has essential structural functions in the septate junctions and developmental functions in embryonic and adult epithelial cells. Mol. Biol. Cell. 9, 3505–3519.

Laprise, P., Lau, K.M., Harris, K.P., Silva-Gagliardi, N.F., Paul, S.M., Beronja, S., Beitel, G.J., McGlade, C.J., Tepass, U., 2009. Yurt, Coracle, Neurexin IV and the $Na^{(+)}$, $K^{(+)}$-ATPase form a novel group of epithelial polarity proteins. Nature 459, 1141–1145.

Legendre, F., Whiting, M.F., Bordereau, C., Cancello, E.M., Evans, T.A., Grandcolas, P., 2008. The phylogeny of termites (Dictyoptera: Isoptera) based on mitochondrial and nuclear markers: implications for the evolution of the worker and pseudergate castes, and foraging behaviors. Mol. Phylogenet. Evol. 48, 615–627.

Lingrel, J.B., Kuntzweiler, T., 1994. Na^+, $K^{(+)}$-ATPase. J. Biol. Chem. 269, 19659–19662.

Lingrel, J.B., Orlowski, J., Shull, M.M., Price, E.M., 1990. Molecular genetics of Na, K-ATPase. Prog. Nucleic Acid Res. Mol. Biol. 38, 37–89.

Lingrel, J.B., Van Huysse, J., O'Brien, W., Jewell-Motz, E., Askew, R., Schultheis, P., 1994. Structure-function studies of the Na, K-ATPase. Kidney Int. Suppl. 44, S32–S39.

Lopina, O.D., 2001. Interaction of Na, K-ATPase catalytic subunit with cellular proteins and other endogenous regulators. Biochemistry 66, 1122–1131 (Mosc).

Maestro, O., Cruz, J., Pascual, N., Martin, D., Belles, X., 2005. Differential expression of two RXR/ultraspiracle isoforms during the life cycle of the hemimetabolous insect Blattella germanica (Dictyoptera, Blattellidae). Mol. Cell. Endocrinol. 238, 27–37.

Martín-Blanco, E., Gampel, A., Ring, J., Virdee, K., Kirov, N., Tolkovsky, A.M., Martinez-Arias, A., 1998. Puckered encodes a phosphatase that mediates a feedback loop regulating JNK activity during dorsal closure in Drosophila. Genes Dev. 12, 557–570.

Mobasheri, A., Avila, J., Cozar-Castellano, I., Brownleader, M.D., Trevan, M., Francis, M.J., Lamb, J.F., Martin-Vasallo, P., 2000. Na^+, K^+-ATPase isozyme diversity; comparative biochemistry and physiological implications of novel functional interactions. Biosci. Rep. 20, 51–91.

Munderloh, U.G., Kurtti, T.J., 1989. Formulation of medium for tick cell culture. Exp. Appl. Acarol. 7, 219–229.

Noguchi, S., Mishina, M., Kawamura, M., Numa, S., 1987. Expression of functional ($Na^+ + K^+$)-ATPase from cloned cDNAs. FEBS Lett. 225, 27–32.

O'Donnell, M., Sharda, R., 1994. Membrane potential and pH regulation in vitellogenic oocytes of an insect, Rhodnius prolixus. Physiol. Zool. 67, 7–28.

Okamura, H., Yasuhara, J.C., Fambrough, D.M., Takeyasu, K., 2003. P-type ATPases in Caenorhabditis and Drosophila: implications for evolution of the P-type ATPase subunit families with special reference to the Na, K-ATPase and H, K-ATPase subgroup. J. Membr. Biol. 191, 13–24.

Oshima, K., Fehon, R.G., 2011. Analysis of protein dynamics within the septate junction reveals a highly stable core protein complex that does not include the basolateral polarity protein discs large. J. Cell. Sci. 124, 2861–2871.

Paul, S.M., Palladino, M.J., Beitel, G.J., 2007. A pump-independent function of the Na, K-ATPase is required for epithelial junction function and tracheal tube-size control. Development 134, 147–155.

Pfaffl, M.W., Horgan, G.W., Dempfle, L., 2002. Relative expression software tool (REST) for group-wise comparison and statistical analysis of relative expression results in real-time PCR. Nucleic Acids Res. 30, e36.

Piulachs, M.D., Maestro, J.L., Belles, X., 1992. Juvenile hormone production and accessory reproductive gland development during sexual maturation of male Blattella germanica (L.) (Dictyoptera, Blattellidae). Comp. Biochem. Physiol. A Comp. Physiol., 477–480.

Piulachs, M.D., Pagone, V., Belles, X., 2010. Key roles of the broad-complex gene in insect embryogenesis. Insect Biochem. Mol. Biol. 40, 468–475.

Pszczolkowski, M.A., Peterson, A., Srinivasan, A., Ramaswamy, S.B., 2005. Pharmacological analysis of ovarial patency in Heliothis virescens. J. Insect Physiol. 51, 445–453.

Sevala, V.L., Davey, K.G., 1989. Action of juvenile hormone on the follicle cells of Rhodnius prolixus: evidence for a novel regulatory mechanism involving protein kinase C. Experientia 45, 355–356.

Shyjan, A.W., Cena, V., Klein, D.C., Levenson, R., 1990a. Differential expression and enzymatic properties of the Na^+, $K^{(+)}$-ATPase alpha 3 isoenzyme in rat pineal glands. Proc. Natl. Acad. Sci. U S A 87, 1178–1182.

Shyjan, A.W., Gottardi, C., Levenson, R., 1990b. The Na, K-ATPase beta 2 subunit is expressed in rat brain and copurifies with Na, K-ATPase activity. J. Biol. Chem. 265, 5166–5169.

Shyjan, A.W., Levenson, R., 1989. Antisera specific for the alpha 1, alpha 2, alpha 3, and beta subunits of the Na, K-ATPase: differential expression of alpha and beta subunits in rat tissue membranes. Biochemistry 28, 4531–4535.

Sun, B., Salvaterra, P.M., 1995a. Characterization of Nervana, a Drosophila melanogaster neuron-specific glycoprotein antigen recognized by anti-horseradish peroxidase antibodies. J. Neurochem. 65, 434–443.

Sun, B., Salvaterra, P.M., 1995b. Two Drosophila nervous system antigens, Nervana 1 and 2, are homologous to the beta subunit of Na^+, $K^{(+)}$-ATPase. Proc. Natl. Acad. Sci. U S A 92, 5396–5400.

Sun, B., Wang, W., Salvaterra, P.M., 1998. Functional analysis and tissue-specific expression of Drosophila Na^+, K^+-ATPase subunits. J. Neurochem. 71, 142–151.

Takeyasu, K., Kawakami, K., 1989. Na^+, $K^{(+)}$-ATPase: genes, expression and membrane insertion. Seikagaku 61, 394–401.

Treiblmayr, K., Pascual, N., Piulachs, M., Keller, T., Belles, X., 2006. Juvenile hormone titer versus juvenile hormone synthesis in female nymphs and adults of the German cockroach, Blattella germanica. J. Insect Sci. 6, 7.

Vagin, O., Tokhtaeva, E., Sachs, G., 2006. The role of the beta1 subunit of the Na, K-ATPase and its glycosylation in cell–cell adhesion. J. Biol. Chem. 281, 39573–39587.

Ward, R.E.t., Lamb, R.S., Fehon, R.G., 1998. A conserved functional domain of Drosophila coracle is required for localization at the septate junction and has membrane-organizing activity. J. Cell. Biol. 140, 1463–1473.

Watts, A.G., Sanchez-Watts, G., Emanuel, J.R., Levenson, R., 1991. Cell-specific expression of mRNAs encoding Na^+, $K^{(+)}$-ATPase alpha- and beta-subunit isoforms within the rat central nervous system. Proc. Natl. Acad. Sci. U S A 88, 7425–7429.

Xu, P., Sun, B., Salvaterra, P.M., 1999. Organization and transcriptional regulation of Drosophila $Na^{(+)}$, $K^{(+)}$-ATPase beta subunit genes: Nrv1 and Nrv2. Gene 236, 303–313.

Zeitlinger, J., Kockel, L., Peverali, F.A., Jackson, D.B., Mlodzik, M., Bohmann, D., 1997. Defective dorsal closure and loss of epidermal decapentaplegic expression in Drosophila fos mutants. EMBO J. 26, 7393–7401.